ARTICLE

# TDDFT Study on Different Sensing Mechanisms of Similar Cyanide Sensors Based on Michael Addition Reaction

Guang-yue Li[a,b*], Ping Song[a], Guo-zhong He[a]

*a. State Key Laboratory of Molecular Reaction Dynamics, Dalian Institute of Chemical Physics, Chinese Academy of Sciences, Dalian 116023, China*
*b. Graduate School of the Chinese Academy of Sciences, Beijing 100049, China*

(Dated: Received on March 2, 2011; Accepted on April 11, 2011)

The solvents and substituents of two similar fluorescent sensors for cyanide, 7-diethylamino-3-formylcoumarin (sensor **a**) and 7-diethylamino-3-(2-nitrovinyl)coumarin (sensor **b**), are proposed to account for their distinct sensing mechanisms and experimental phenomena. The time-dependent density functional theory has been applied to investigate the ground states and the first singlet excited electronic states of the sensor as well as their possible Michael reaction products with cyanide, with a view to monitoring their geometries and photophysical properties. The theoretical study indicates that the protic water solvent could lead to final Michael addition product of sensor **a** in the ground state, while the aprotic acetonitrile solvent could lead to carbanion as the final product of sensor **b**. Furthermore, the Michael reaction product of sensor **a** has been proved to have a torsion structure in its first singlet excited state. Correspondingly, sensor **b** also has a torsion structure around the nitrovinyl moiety in its first singlet excited state, while not in its carbanion structure. This could explain the observed strong fluorescence for sensor **a** and the quenching fluorescence for the sensor **b** upon the addition of the cyanide anions in the relevant sensing mechanisms.

**Key words:** Sensor, Fluorescence, Cyanide, Sensing mechanism, Time-dependent density functional theory, Michael addition reaction

## I. INTRODUCTION

Cyanide anions are widespread in surface water from biological source [1] and widely used in many industries [2] involving gold mining, electroplating and metallurgy. However, even small amounts of the cyanide anion are extremely harmful to living creatures. For example, $LD_{50}$ (estimated dose that is lethal to 50% of the exposed population) of hydrogen cyanide can be as low as 1.0 mg/kg body weight for humans [3]. Cyanide anions can make the cells of a living creature unable to use oxygen, primarily through the inhibition of cytochrome c oxidase [4]. Furthermore, exposure to lower levels of cyanides over a long period will lead to a rise of blood cyanide levels, which could result in a variety of symptoms [5]. Therefore, any accidental release of cyanides can result in serious environmental damage. There is thus an exigent need for cyanide-selective sensors.

Cyanide anion is a weaker hydrogen-bond acceptor, but it also has strong coordination ability and strong nucleophility. Many cyanide sensor are designed based on the above characters. Gimeno *et al.* synthesized two new azophenyl thiourea sensors [6] to detect cyanide based on the hydrogen-bond interaction, and they showed good selectivity over other anions in both solution and supported onto $Al_2O_3$ nanostructured films. Ganesh *et al.* used the Cu-complex as the cyanide sensor system to design an SAM-modified gold electrode [7], in which the copper ions could be removed by cyanide anions. Lee *et al.* reported 8-formyl-7-hydroxycoumarin as a fluorescent cyanide sensor using a nucleophilic addition reaction [8], and it is found that the sensor selectively displayed a dramatic change in fluorescence intensity in response to cyanide anions in water at biological pH. Especially, the Michael addition reaction is one of the most important ways underpinning sensors designed to detect cyanide among the nucleophilic reactions [9−12]. The Michael addition reaction is the thermodynamically controlled 1,4-addition (or conjugate addition) of conjugation-stabilized carbanions. The reaction donors are strong carbon acids such as cyanides and malonates, and the acceptors are usually $\alpha,\beta$-unsaturated carbonyl compounds. In other words, a cyanide anion can react with the $\alpha,\beta$-unsaturated carbonyl compound in a conjugate addition reaction. Proton abstraction from protonated base (or solvent) by the enolate structure is the final step.

Fluorescent sensors can quantificationally recognize species, in which the fluorescence intensity and emission

*Author to whom correspondence should be addressed. E-mail: gyli@dicp.ac.cn, Tel.: +86-411-84379692. FAX: +86-411-84675584

 

wavelength is easily and sensitively monitored. So, fluorescent sensors for cyanide have been actively investigated in recent years [9−18]. Several spectroscopic techniques, such as time-resolved fluorescence spectroscopy, can study the sensing mechanism [19], but they provide only indirect information about photophysical properties and geometries. To further understand the sensing mechanism, we need to use density functional theory (DFT) and time-dependent density functional theory (TD-DFT) to clarify fundamental aspects concerning the mechanism in the $S_0$ and $S_1$ states, respectively. As mentioned above, although fluorescent sensors for cyanide have been synthesized and some mechanisms of them have been supposed in above report [19], the detailed sensing mechanism has been seldom theoretically explained to the best of our knowledge.

Recently, Kim *et al.* reported two fluorescent sensors for the cyanide anion (**a** and **b**, as shown in Scheme 1) using the coumarin derivatives as the fluorophores [9, 10]. They considered that cyanides can be added to the 4-position of the coumarin moiety through Michael addition reaction, which is doubly activated by both the formyl of **a** (or nitro of **b**) and the coumarinyl carbonyl group. Then, the added cyanide groups could change the aromatic stability and lead to a fluorescence change of the fluorophore. It is interesting that the authors provided different mechanisms for the cyanide sensors with similar structures. Accordingly, it is important to understand the detailed sensing mechanism of the interaction between the sensor and anions because of its clearly crucial role in different solvents. In the present work, we report a theoretical study concerning the sensors (see Scheme 1), which may represent a new candidate for investigating the mechanism of cyanide reorganization. The present calculation aims to provide an explanation on the sensing mechanisms of the cyanide sensors. In particular, we have focused our attention on the mechanism relating to the different solvents. Meanwhile, we have extensively studied the photophysics and photochemistry of these systems.

## II. COMPUTATIONAL DETAILS

All calculations on electronic structures were carried out using the Gaussian 09 program suite [20]. Geometry optimizations for the ground state and the first singlet electronic excited state were performed using DFT and TD-DFT methods, respectively. A test with a series of functionals (BP86, BLYP, PW91, B3P86, B3LYP and B3PW91) was performed for photochemical properties for the sensor **a**. As a result, B3P86 functional [21−25], Becke's three-parameter hybrid exchange functional with the non-local correlation provided by Perdew 86, was the more reasonable choice to be in good accordance with the experimental results and not time-consumption. Then it was used in both the DFT and TD-DFT methods in the sequential work. The triple-$\zeta$ valence quality with one set of polarization functions (TZVP) [26] was chosen as basis sets throughout, which is an appropriate basis set for such ionic organic compounds [27−31]. No constrains for symmetry, bonds, angles, or dihedral angles were applied in the geometry optimization calculations. To evaluate the solvent effect, water and acetonitrile were employed as solvent in the SCRF calculations by using the conductor-like screening model (COSMO) method [32]. All of the local minima were confirmed by the absence of an imaginary mode in vibrational analysis calculations.

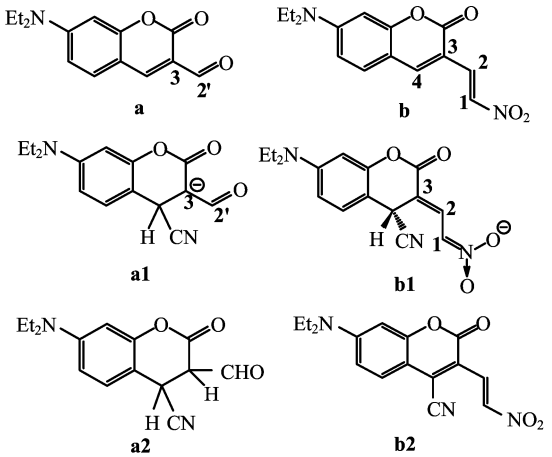


Scheme 1 Structures of **a**, **b**, **a1**, **b1**, **a2**, and **b2**.

## III. RESULTS AND DISCUSSION

### A. Optimized structures in the ground state

Typically, both the sensor **a** and sensor **b** can react with cyanide anion to form the enolate-type anions **a1** and **b1** based on Michael addition reaction. In Ref.[10], sensor **a** has been synthesized in water and the spectra have been measured in HEPES buffer (pH=7.4). Herein, we supposed that proton-abstracting product **a2** of the enolate **a1** from solvent should be the final reaction step. In Ref.[9], **b** has been synthesized and measured in aprotic acetonitrile solvent, and the molecule **b2** was thought to be the final product upon adding cyanide anions.

Accordingly, the ground-state structures of the sensor **a** and **b**, as well as **a1**, **b1**, **a2**, and **b2** (shown in Scheme 1), were obtained using the B3P86 functional with TZVP basis set. To evaluate the solvent effect, acetonitrile and water were respectively used in the calculations according to the COSMO solvation model. We started the optimization from a set of initial configurations in order to avoid local minima and the global minima of these molecules only have real frequencies. In **a**, **b**, and **a2**, all the atoms are nearly on the same plane except their two ethyl groups. The cyanide-addition product **a1** and **b1** are both fold-shape molecules, the

DOI:10.1088/1674-0068/24/03/305-310 

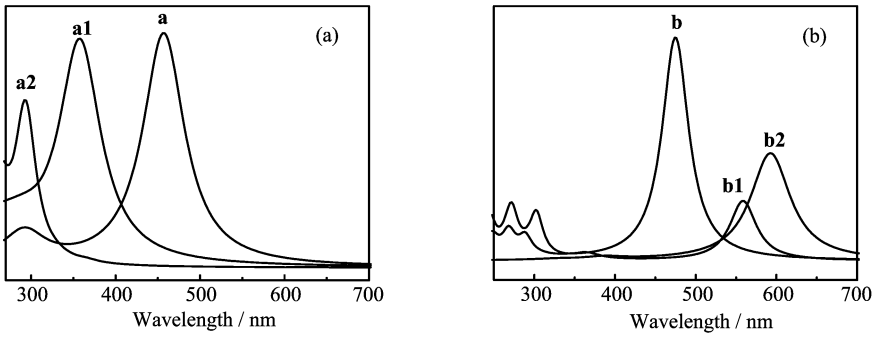


FIG. 1 Calculated absorption spectra of (a) (**a**, **a1**, and **a2**) and (b) (**b**, **b1**, and **b2**) by the TD-DFT method.

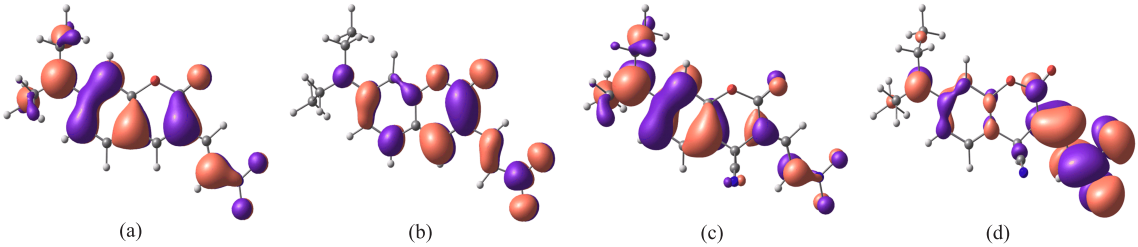


FIG. 2 HOMOs and LUMOs of sensor obtained from DFT/B3P86/TZVP calculations. (a) HOMO of **b**, (b) LUMO of **b**, (c) HOMO of **b1**, and (d) LUMO of **b1**.

angles of which are both approximately 150°.

### B. Absorption spectra and molecular orbital

We calculated the absorption spectra of all the molecules using the TD-DFT/B3P86/TZVP method with COSMO solvation model, and compared them with the experimental data [9, 10]. Figure 1(a) shows the calculated absorption spectra of **a**, **a1**, and **a2**. The maximum absorption band of sensor **a** appears around 457 nm, which well reproduces the experimental UV/Vis band of **a** at 446 nm. Furthermore, **a1** and **a2** show their computational maxima at 357 and 292 nm respectively, and the latter corresponds to the experimental absorption band of the sensor **a** upon the addition of cyanide (282 nm). That is to say, the product of the sensor **a** reacting with cyanide anion in water is **a2** instead of **a1**. Similarly, the computational absorption bands of **b** and **b1** well reproduce the experimental data. It indicates that the final Michael addition product of sensor **b** is negative molecule **b1**. Thus, the preliminary conclusions could be deduced from the comparison between the calculated absorption spectra and the corresponding experimental UV/Vis spectra. Both sensor **a** and sensor **b** can react with cyanide anions, but the final products are different due to their different solvents. The protic water solvent leads to the addition product **a2**, and the aprotic acetonitrile solvent leads to the anion product **b1**.

The molecular orbitals involved in the $S_0$-$S_1$ transitions have been calculated for all the molecules, and each of them is proved to be a dominant $\pi\pi^*$-type transition. In sensor **b**, the $S_0$-$S_1$ transition is from the highest occupied molecular orbital (HOMO) to the lowest unoccupied molecular orbital (LUMO). As shown in Fig.2, the LUMO of **b** is generally with the antibonding character of the $C_2-C_3$ bond. It reveals that the conformation of the excited state of sensor **b** may be in torsion state around the $C_2-C_3$ bond, the similar phenomenon has been reported recently [33]. Similarly, the molecule **b1** shows the antibonding character of the $C_1-C_2$ bond in LUMO. Herein, we predicted that there are more than one local stable structure for **b** and **b1** and they could result in structural torsion in the $S_1$ state.

### C. Optimized structures in the first singlet excited state

Figure 3 shows the optimized $S_1$-state structures of **a**, **a2**, **b** and **b1**. The sensor **a** keeps the similar structure in the $S_1$ state to that in the $S_0$ state. The molecule **a2** shows a different structure. The aldehyde group of **a2** exists as an axial bond in the $S_1$ state rather than an equatorial one in the $S_0$ state. That is to say, relaxation to the stable geometry of **a2** may involve an obvious configurational change upon excitation. This could explain that the green fluorescence of sensor **a** was quenched in the solution of cyanide anion. Moreover, we found that the sensor **b** has three local minima (E-form, V-form, and Z-form) and **b1** has two (Z-form and V-form) in their $S_1$ state. The $S_1$-state global minimum structure of **b** is corresponding to the V-form,

DOI:10.1088/1674-0068/24/03/305-310 

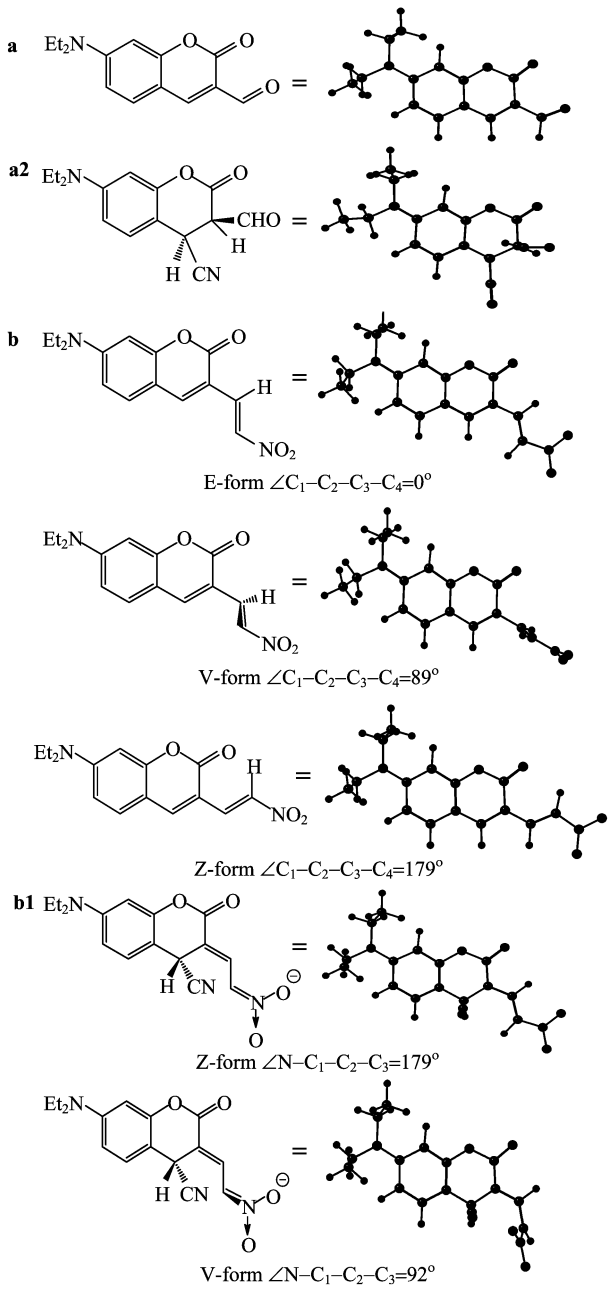


FIG. 3 $S_1$-state structures of **a**, **a2**, **b**, and **b1** and specific dihedral angles by the TD-DFT method.

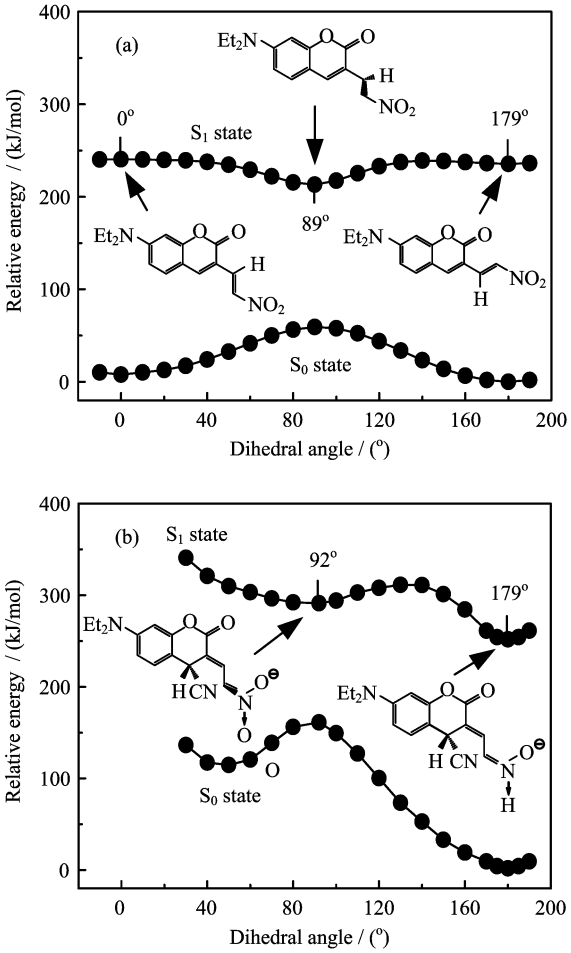


FIG. 4 Potential-energy curves of the $S_0$ and $S_1$ states for (a) sensor **b** and (b) **b1** as functions of the corresponding dihedral angles in the $S_1$ state, calculated at the TD-DFT/B3LYP/TZVP level with COSMO solvation model. The energies of $S_0$ state have been calculated at the optimized geometries of the $S_1$ state.

by twisting the nitro group onto a plane perpendicular to that of the coumarin group. But the E-form structure of **b1** is its global minimum, the energy of which is lower than that of V-form. That is to say, the geometry of **b1** in the $S_1$ state is very similar to that in the $S_0$ state. So, we surmise that the $S_1$ state of **b** is a twisted excited state and that of **b1** is a local excited state, which could be responsible for the strong fluorescence of the sensor **b** upon adding the cyanide anions.

We also obtained the excited-state structures of **a**, **a2**, **b**, and **b1** at TD-DFT/B3P86/TZVP level with COSMO solvation model. For calculations on **a**, we used the initial configurations obtained from the ground-state optimizations. As mentioned above, it has been demonstrated that both **b** and **b1** may have torsional structures in their $S_1$ states. For this reason, we used a set of possible structures as the initial configurations for the $S_1$-state optimization. Their local minima only have real frequencies. The $S_1$-$S_0$ vertical emission energies of **a** and **b1** determined on the basis of the TD-DFT calculation were found to well reproduce the experimental fluorescence emission energies [9, 10] (see Fig.4).

### D. The $S_1$ potential-energy curves of sensor b and b1

Figure 4 provides an overview of the potential-energy curves of **b** and **b1** as functions of twist angle in the $S_1$ states. The energies of the $S_1$ states were optimized for the specific dihedral angles ($\angle C_1{-}C_2{-}C_3{-}C_4$ for

DOI:10.1088/1674-0068/24/03/305-310 

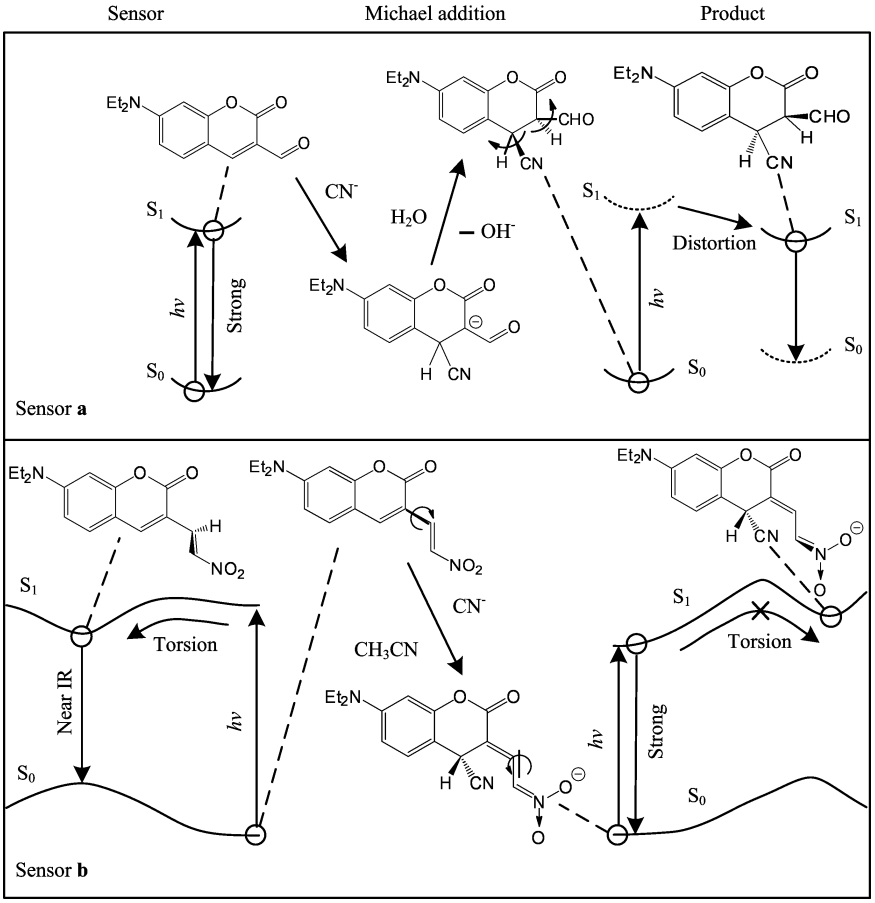


Scheme 2 Entire sensing processes for the sensor **a** and sensor **b** for recognizing cyanide anion.

**b** and $\angle N-C_1-C_2-C_3$ for **b1**) obtained at the TD-DFT/B3P86/TZVP level using the COSMO solvation model. The $S_0$-energy profiles of the twisting paths were calculated based on the geometries of the $S_1$ states.

As shown in Fig.4(a), **b** shows a barrierless potential-energy curve in the $S_1$ state, the energy of which decreases along the dihedral angle from 0° to 89°. This provides a possible explanation for the fluorescence quenching of **b**. In contrast, Fig.4(b) shows the distinct $S_1$ potential curve of **b1**, which exhibits a barrier of approximately 50 kJ/mol. As indicated in the excited-state geometry, the $S_1$-$S_0$ vertical emission energy of the E-form **b1** shows minor difference from the experimental fluorescence wavelength. This indicates that **b1** prefers to return to the $S_0$ state through the strong emission of fluorescence rather than by surmounting the potential barrier in the potential-energy curve. Compared with the potential-energy curves of **b**, the local excited-state structure of **b1** can explain the dramatic enhancement in fluorescence intensity seen in the presence of cyanide anions.

### E. Sensing mechanism

Scheme 2 provides the information of the sensing mechanisms in details. The results we presented have explained the two opposite fluorescent phenomena between the sensors **a** and **b** during the sensing process. Sensor **a** and its Michael addition product **a2** show different behaviors in their $S_0$ and $S_1$ states. The local excited state of **a** is not involved in any obvious structural changes, which is responsible for the strong fluorescence of the sensor **a**. Cyanide anion is deposited on the 4-position of the coumarin moiety of sensor **a** in its $S_0$ state through Michael addition reaction to afford the carbanion **a1**. Subsequently, **a1** is protonated by water to afford the addition product **a2**. In the $S_1$ state of **a2**, a structural distortion takes place, whereby the non-radiative deactivation can occur. This could explain the fluorescence quenching of **a2** observed experimentally [9]. Correspondingly, the sensing mechanism of the sensor **b** is delineated as follows. In the $S_1$ state, sensor **b** can undergo a torsion process over a very low potential barrier. Then, near-infrared emission or non-radiative deactivation leads to the weak fluorescence of **b** to the extent of experimental observation. Cyanide anion is also added to sensor **b** in its $S_0$ state through Michael addition reaction to afford the carbanion **b1**, which exhibits an $S_1$-state structure similar to the $S_0$-state structure. In this geometry, the $S_1$-$S_0$ energy gap confirms to the experimental fluorescence emission energy. This could explain the enhanced fluorescence of

DOI:10.1088/1674-0068/24/03/305-310 

sensor **b** upon addition of cyanide anion. Therefore, the sensor **a** and **b** can be used to sense cyanide anions by monitoring the changes in their fluorescence spectra.

## IV. CONCLUSION

We have verified theoretically that two sensor **a** and **b** have different mechanisms of sensing cyanide anions. The theoretical study has indicated that sensor **a** shows similar structures in the $S_0$ and $S_1$ state to induce strong fluorescence. Cyanide anion can react with sensor **a** through Michael addition reaction in protic water solution. The $\alpha$,$\beta$-addition product undergoes the structural change in the $S_1$ state, which is responsible for the fluorescence quenching of the sensor **a** when adding cyanide anions in the water solution. Sensor **b** has been proved to have a torsion structure in its $S_1$ state. In the aprotic acetonitrile solvent, cyanide anion could also add to the sensor **b** through Michael addition reaction to afford a carbanion as the final product. The carbanion goes against the structural torsion and enhances the fluorescence. In summary, the different solvents and substituents of sensor **a** and sensor **b** result in different Michael addition products with cyanide, then causing the different sensing mechanisms and consequently the fluorescence spectra change. This will provide another way to synthesis new sensors for cyanide anion.

## V. ACKNOWLEDGMENTS

This work was supported by the National Key Basic Research Special Foundation (No.2007CB815202 and No.2009CB220010) and the National Natural Science Foundation of China (No.20833008).

[1] Z. C. Xu, X. Q. Chen, H. N. Kim, and J. Y. Yoon, Chem. Soc. Rev. **39**, 127 (2010).
[2] C. Young, L. Tidwell, and C. Anderson, *Cyanide: Social, Industrial, and Economic Aspects*, Warrendale, PA: Minerals, Metals, and Materials Society, 49 (2001).
[3] S. I. Baskin and T. G. Brewer, *Medical Aspects of Chemical and Biological Warfare*, Washington, DC: TMM Publication, 271 (1997).
[4] B. Vennesland, E. E. Conn, C. J. Knownles, J. Westly, and F. Wissing, *Cyanide in Biology*, London: Academic Press, 133 (1981).
[5] D. Nhassico, H. Muquingue, J. Cliff, A. Cumbana, and J. H. Bradbury, J. Sci. Food Agric. **88**, 204 (2008).
[6] N. Gimeno, X. Li, J. R. Durrant, and R. Vilar, Chem. Eur. J. **14**, 3006 (2008).
[7] V. Ganesh, M. P. C. Sanz, and J. C. Mareque-Rivas, Chem. Commun. 5010 (2007).
[8] K. S. Lee, H. J. Kim, G. H. Kim, I. Shin, and J. I. Hong, Org. Lett. **10**, 49 (2008).
[9] G. J. Kim and H. J. Kim, Tetrahedron Lett. **51**, 185 (2010).
[10] G. J. Kim and H. J. Kim, Tetrahedron Lett. **51**, 2914 (2010).
[11] S. J. Hong, J. Yoo, S. H. Kim, J. S. Kim, J. Yoon, and C. H. Lee, Chem. Commun. 189 (2009).
[12] S. Park and H. J. Kim, Chem. Commun. **46**, 9197 (2010).
[13] Z. Dai and E. M. Boon, J. Am. Chem. Soc. **132**, 11496 (2010).
[14] M. R. Ajayakumar and P. Mukhopadhyay, Org. Lett. **12**, 2646 (2010).
[15] Y. Sun, Y. Liu, M. Chen, and W. Guo, Talanta **80**, 996 (2009).
[16] J. Wang and C. S. Ha, Tetrahedron **66**, 1846 (2010).
[17] T. Ábalos, D. Jiménez, M. Moragues, S. Royo, R. Martínez-Máñez, F. Sancenón, J. Soto, A. M. Costero, M. Parra, and S. Gil, Dalton Trans. **39**, 3449 (2010).
[18] S. S. Sun, and A. J. Lees, Chem. Commun. 1687 (2000).
[19] A. S. Klymchenko, D. A. Yushchenko, and Y. Mély, J. Photoch. Photobio. A **192**, 93 (2007).
[20] M. J. Frisch, G. W. Trucks, H. B. Schlegel, G. E. Scuseria, M. A. Robb, J. R. Cheeseman, G. Scalmani, V. Barone, B. Mennucci, G. A. Petersson, H. Nakatsuji, M. Caricato, X. Li, H. P. Hratchian, A. F. Izmaylov, J. Bloino, G. Zheng, J. L. Sonnenberg, M. Hada, M. Ehara, K. Toyota, R. Fukuda, J. Hasegawa, M. Ishida, T. Nakajima, Y. Honda, O. Kitao, H. Nakai, T. Vreven, J. A. Montgomery Jr., J. E. Peralta, F. Ogliaro, M. Bearpark, J. J. Heyd, E. Brothers, K. N. Kudin, V. N. Staroverov, R. Kobayashi, J. Normand, K. Raghavachari, A. Rendell, J. C. Burant, S. S. Iyengar, J. Tomasi, M. Cossi, N. Rega, J. M. Millam, M. Klene, J. E. Knox, J. B. Cross, V. Bakken, C. Adamo, J. Jaramillo, R. Gomperts, R. E. Stratmann, O. Yazyev, A. J. Austin, R. Cammi, C. Pomelli, J. W. Ochterski, R. L. Martin, K. Morokuma, V. G. Zakrzewski, G. A. Voth, P. Salvador, J. J. Dannenberg, S. Dapprich, A. D. Daniels, Ö. Farkas, J. B. Foresman, J. V. Ortiz, J. Cioslowski, and D. J. Fox, *Gaussian 09*, *Revision A.1*, Wallingford CT: Gaussian, Inc., (2009).
[21] A. D. Becke, J. Chem. Phys. **98**, 5648 (1993).
[22] P. A. M. Dirac, Proc. Royal Soc. (London) A **123**, 714 (1929).
[23] S. H. Vosko, L. Wilk, and M. Nusair, Can. J. Phys. **58**, 1200 (1980).
[24] A. D. Becke, Phys. Rev. A **38**, 3098 (1988).
[25] J. P. Perdew, Phys. Rev. B **33**, 8822 (1986).
[26] O. Treutler and R. Ahlrichs, J. Chem. Phys. **102**, 346 (1995).
[27] G. J. Zhao and K. L. Han, J. Phys. Chem. A **111**, 9218 (2007).
[28] G. J. Zhao and K. L. Han, Biophys. J. **94**, 38 (2008).
[29] G. J. Zhao, J. Y. Liu, L. C. Zhou, and K. L. Han, J. Phys. Chem. B **111**, 8940 (2007).
[30] T. S. Chu, Y. Zhang, and K. L. Han, Int. Rev. Phys. Chem. **25**, 201 (2006).
[31] G. J. Zhao and K. L. Han, J. Phys. Chem. A **113**, 14329 (2009).
[32] A. Klamt and G. Schüürmann, J. Chem. Soc. Perkin Trans. **2**, 799 (1993).
[33] G. J. Zhao and K. L. Han, J. Phys. Chem. A **111**, 2469 (2007).

DOI:10.1088/1674-0068/24/03/305-310 